

Mesons at large N_c from lattice QCD

Gunnar S. Bali

Institut für Theoretische Physik, Universität Regensburg, 93040 Regensburg, Germany
E-mail: gunnar.bali@physik.uni-regensburg.de

Francis Bursa

Rudolf Peierls Centre for Theoretical Physics, University of Oxford,
1 Keble Road, Oxford OX1 3NP, U.K.
E-mail: f.bursa1@physics.ox.ac.uk

ABSTRACT: We calculate the pion and ρ meson masses in quenched $SU(N)$ gauge theories for $N = 2, 3, 4$ and 6. Extrapolating these results to the chiral and large- N limits, we find $m_\rho = (1.670 \pm 0.024)\sqrt{\sigma} = (741 \pm 11)$ MeV for the ρ meson mass at a fixed lattice spacing $a \approx 0.093$ fm. We estimate a continuum value, $m_\rho = (786 \pm 22)$ MeV, where we use the value $\sigma = 1$ GeV/fm $\approx (444 \text{ MeV})^2$ for the string tension. We find $1/N^2$ corrections to be small and we compare our results to predictions from AdS/QCD.

KEYWORDS: Lattice QCD, $1/N$ Expansion, AdS-CFT Correspondence.

Contents

1. Introduction	1
2. Simulation parameters and lattice methods	2
3. Results	4
3.1 Extracting masses from correlation functions	4
3.2 Finite size effects	6
3.3 Determination of the critical hopping parameter	8
3.3.1 κ_c at finite N	8
3.3.2 κ_c in the large- N limit	9
3.4 The ρ meson mass	10
3.4.1 m_ρ at finite N	10
3.4.2 m_ρ in the large- N limit	10
3.5 Excited states	12
4. The continuum limit	12
5. Summary and Discussion	14

1. Introduction

Numerical simulations of QCD in lattice regularization (Lattice QCD) are the standard way to derive low energy aspects of the phenomenology of strongly interacting elementary particles, directly from the QCD Lagrangian. Adding conformal invariance via supersymmetry or sending the number of colours N from three to infinity are popular ways of turning some aspects of non-perturbative QCD analytically tractable. Such extensions are in particular also necessary to connect supergravity predictions to properties of induced four dimensional quantum field theories on the boundary of anti-de Sitter space [1] (AdS/CFT correspondence or AdS/QCD [2, 3, 4]).

Pure $SU(N)$ gauge theories have been studied extensively on the lattice and, among other quantities, the glueball spectra, string tensions [5], \overline{MS} Λ -parameters [6] and deconfinement transition temperatures [7] are well-established. These pure Young-Mills results demonstrate that $1/N^2$ corrections are already below the 10 % level at $N = 3$. Nothing is known as yet for full QCD at $N > 3$, including n_F flavours of sea quarks, in which case corrections to the meson spectrum are expected to be only suppressed by factors n_F/N .

Here, as a first step in this direction, we study the meson spectrum in the quenched approximation for $N = 2, 3, 4$ and 6. While this alone will not allow us to quantify the

difference between $N = 3$ and the large- N limit of full QCD, the quenched and the full theory will share the same large- N limit where sea quark loops are suppressed for any finite number of quark flavours [8].

Obtaining large- N results that are close to existing full $N = 3$ QCD results (or indeed to real world experiment) will help us to understand why the quenched approximation (and even the naive quark model) works remarkably well in many cases [9]. The large- N expansion is also a powerful tool to reduce the number of low energy constants in chiral effective field theories [10] and we wish to understand in what cases *three* can be regarded as a large number and under what circumstances not. Moreover, QCD in the planar limit is an interesting quantum field theory in itself. Last but not least, only in this limit the AdS/QCD correspondence can work.

First exploratory simulations of the pion masses in SU(17) and SU(19) were performed by Kiskis, Narayanan and Neuberger [11] some time ago, employing overlap fermions. Preliminary results for the π and ρ meson masses using the Wilson gauge and fermion actions for $N = 2, 3, 4$ and 6 were presented by us at Lattice 07 [12]. The present article concludes this study. Recently, Del Debbio *et al.* [13], obtained the π and ρ meson masses as well, using the same action at the same N -values, at a somewhat coarser lattice spacing than ours. This coincidence gives us some control of the continuum limit.

This article is organised as follows: in section 2 we introduce the methods employed in the simulation. In section 3 we describe our analysis methods and present the results. We discuss finite volume corrections, the N -dependence of the additive quark mass renormalization and the ρ meson mass as a function of the π mass at large N . In section 4 we relate our results to those of Ref. [13] and perform the continuum limit extrapolation, before we conclude the article with a discussion in section 5.

2. Simulation parameters and lattice methods

We use the software package *Chroma* [14], to carry out our simulations which we have adapted to work for a general number of colours N .

We use the Wilson plaquette gauge action,

$$S_g = \beta \sum_{\square} \left(1 - \frac{1}{N} \text{Re Tr } U_{\square} \right), \quad (2.1)$$

where U_{\square} is the product of SU(N) link matrices $U_{x,\mu}$, connecting the site x with the site $x + a\hat{\mu}$, around an elementary plaquette \square . a denotes the lattice spacing and $\hat{\mu}$ a unit vector in μ -direction. We use Wilson fermions with hopping parameter κ ,

$$S_f = \sum_x \psi_x^\dagger \psi_x - \kappa \sum_{x,\mu} \left[\psi_x^\dagger (1 - \gamma_\mu) U_{x,\mu} \psi_{x+a\hat{\mu}} + \psi_x^\dagger (1 + \gamma_\mu) U_{x-a\hat{\mu},\mu}^\dagger \psi_{x-a\hat{\mu}} \right]. \quad (2.2)$$

κ is related to the lattice quark mass m_q by

$$am_q = \frac{1}{2} \left(\frac{1}{\kappa} - \frac{1}{\kappa_c} \right) \quad \text{and} \quad \kappa_c^{-1} = 8 + \mathcal{O}(\beta^{-1}). \quad (2.3)$$

To set the scale, we use the string tension calculations by Lucini *et al.* [15]. We choose the coupling $\beta = 2N/g^2 = 2N^2/\lambda$ such that the infinite-volume string tension in lattice units $a\sqrt{\sigma}$ is the same for each N . We use the value $a\sqrt{\sigma} \approx 0.2093$: for SU(3) this corresponds to $\beta = 6.0175$. λ denotes the 't Hooft coupling in the lattice scheme. At our lattice spacing it converges towards the $N \rightarrow \infty$ value $\lambda \approx 2.78$. Adopting the value $\sigma = 1 \text{ GeV/fm} \approx (444 \text{ MeV})^2$ for the string tension, the lattice spacing is $a \approx 0.093 \text{ fm}$ in each case. The values of $a\sqrt{\sigma}$ [15] used in the fits are very accurate [5], so the mismatch of our lattice spacings in units of the string tension between different N is below the 1 % level.

We have chosen our quark masses (or equivalently our values of κ) in order to match the pion masses $m_\pi/\sqrt{\sigma}$ between the different N -values as closely as possible. These κ -values were estimated by carrying out short exploratory simulations of m_π at different mass points and interpolating.

N	β	$\lambda = 2N^2/\beta$	Volume	κ	n_{conf}
2	2.4645	3.246	$12^3 \times 32$	0.1510	100
			$16^3 \times 32$	0.1457, 0.1480, 0.1500, 0.1510	100
			$24^3 \times 32$	0.1510	100
3	6.0175	2.991	$12^3 \times 32$	0.1547	50
			$16^3 \times 32$	0.1500, 0.1520, 0.1537, 0.1547	50
4	11.028	2.902	$12^3 \times 32$	0.15625	50
			$16^3 \times 32$	0.1520, 0.1540, 0.1554, 0.15625	50
6	25.452	2.829	$12^3 \times 32$	0.15715	50
			$16^3 \times 32$	0.1525, 0.1550, 0.1563, 0.15715	44

Table 1: Simulation parameters. n_{conf} denotes the number of independent gauge configurations.

Our simulation parameters are given in table 1. We carry out most of our calculations on lattices with volume $16^3 \times 32$ in lattice units, corresponding to a spatial extent of ≈ 1.5 fm in physical units. We carry out additional simulations on $12^3 \times 32$ lattices at our lightest quark masses, where finite size effects (FSE) are expected to be largest. In SU(2) we augment this by a $24^3 \times 32$ volume, since FSE are also expected to become larger with smaller N . Indeed, FSE are expected to be *zero* at infinite N , as long as the lattice is kept larger than a critical length l_c [16]. Hence an extrapolation at a fixed finite volume to infinite N will yield the correct $N = \infty$ limit, in spite of any residual FSE we may encounter at finite N .

We calculate correlators using three sources: ‘point’, ‘narrow’ and ‘wide’, and the corresponding three sinks. We employ Jacobi-Gauss smearing [17],

$$\psi'_x = \psi_x + \gamma \sum_i \left(U_{x,i} \psi_{x+a\hat{i}} + U_{x-a\hat{i},i}^\dagger \psi_{x-a\hat{i}} \right), \quad (2.4)$$

with smearing parameter $\gamma = 4$, with 10 iterations for the ‘narrow’ sources and sinks and 60 for the ‘wide’ ones. Prior to this we carry out 10 iterations of spatial APE smearing on

the parallel transporters appearing within eq. (2.4) above [18],

$$U'_{x,i} = \text{Proj}_{\text{SU}(N)} \left[\alpha U_{x,i} + \sum_{j \neq i} \left(U_{x,j} U_{x+a\hat{j},i} U_{x+a\hat{i},j}^\dagger + U_{x-a\hat{j},j}^\dagger U_{x-a\hat{j},i} U_{x+a\hat{i}-a\hat{j},j} \right) \right], \quad (2.5)$$

with smearing parameter $\alpha = 2.5$, where $U_\mu(x)$ is projected back into $\text{SU}(N)$ after each iteration.

We invert the Dirac operator using the Conjugate Gradient (CG) algorithm with even/odd preconditioning. We find the number of CG iterations to be approximately independent of N at a given pion mass. Since each CG matrix-vector multiplication has a cost proportional to N and we have to solve for N different colour sources, the total cost of producing a propagator is proportional to N^2 . Updating a gauge configuration (and also carrying out APE smearing) involves matrix-matrix multiplications and so has a cost proportional to N^3 ; however, for the relatively small values of N we use, the cost of calculating the propagators dominates, so the total computer time spent on generating and analyzing a fixed number of configurations is still roughly proportional to N^2 .

We find that the correlators become less noisy as N increases, so we are able to extract masses with smaller errors from the same number of configurations. We find the errors for a given number of configurations to decrease approximately like $1/\sqrt{N}$ (see tables 2–5). Hence the number of configurations that would be required for equal precision decreases like $1/N$ and the total cost is only proportional to N . A heuristic argument supporting this observed reduction in noise is the increase in the number of degrees of freedom of the statistical system $\propto N^2$ at fixed volume. As noted above, the errors decrease by factors $\simeq 1/\sqrt{N}$ that are somewhat smaller than this best-case $1/N$ scenario.

3. Results

3.1 Extracting masses from correlation functions

As described above, for each channel of interest we calculate cross-correlation matrices $C_{ij}(t) = \langle O_i(t) O_j^\dagger(0) \rangle$, where i, j correspond to the size (‘point’, ‘narrow’ or ‘wide’) of the sources and sinks. To extract masses, we first calculate eigenvectors $\psi_{t_0}^\alpha$ of the generalised eigenvalue problem [19, 20]:

$$C^{-1}(t_0) C(t_0 + a) \psi_{t_0}^\alpha = \lambda_{t_0}^\alpha \psi_{t_0}^\alpha. \quad (3.1)$$

We then project $C(t)$ onto the eigenvector ψ^α that corresponds to the largest eigenvalue λ^α and perform periodic cosh fits, varying the fit ranges, to extract the lowest mass. We also vary t_0 within the range $0 - 2a$; our results are not very sensitive with respect to the value of t_0 . We estimate errors on the masses using the jackknife method.

As an example we show in figure 1 the effective masses for our lightest pion in $\text{SU}(2)$ and $\text{SU}(6)$. We see that there are clear plateaus over a large range of t -values. These plots are typical of those for other N and other masses.

As mentioned above (and as is also visible from figure 1), we find that the correlators become less noisy, and hence the errors on the masses decrease, as N increases. We illustrate

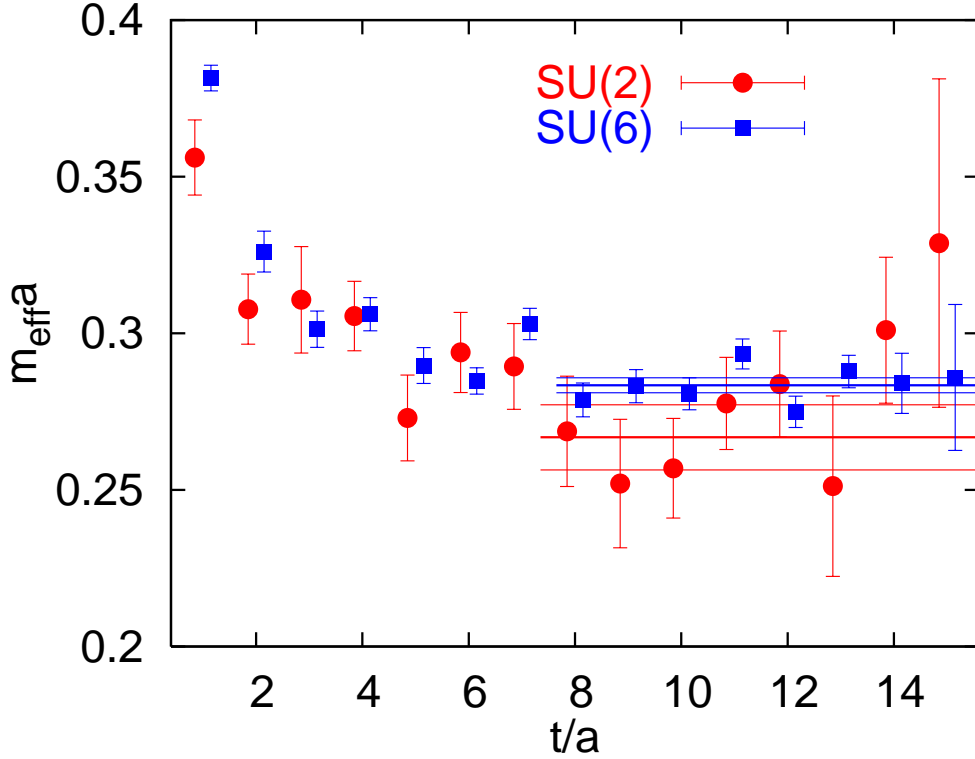


Figure 1: Effective masses and fits for the π ground states at the lightest mass-value for $N = 2$ ($\kappa = 0.1510$, $m_\pi = 1.29(5)\sqrt{\sigma}$) and $N = 6$ ($\kappa = 0.15715$, $m_\pi = 1.35(1)\sqrt{\sigma}$). The lattice volumes were $16^3 \times 32$ in both cases and $t_0 = a$ for $N = 2$ while $t_0 = 2a$ for the more precise SU(6) data.

this in figure 2, where we compare point-point pseudoscalar correlators on individual gauge configurations in SU(3) and SU(6). The pion masses are almost identical, $am_\pi = 0.276(4)$ and $0.283(2)$, respectively, but the scatter between individual configurations, a measure of the noise, is about twice as large in SU(3). This is in agreement with the naive degrees of freedom argument presented above.

κ	Volume	am_π	$m_\pi/\sqrt{\sigma}$	am_ρ	$m_\rho/\sqrt{\sigma}$
0.1457	$16^3 \times 32$	0.559(4)	2.67(2)	0.608(8)	2.90(4)
0.1480	$16^3 \times 32$	0.446(5)	2.13(2)	0.506(10)	2.42(5)
0.1500	$16^3 \times 32$	0.336(7)	1.61(3)	0.428(14)	2.04(7)
0.1510	$12^3 \times 32$	0.305(23)	1.46(11)	0.419(19)	2.00(9)
	$16^3 \times 32$	0.267(10)	1.29(5)	0.392(20)	1.87(10)
	$24^3 \times 32$	0.280(3)	1.34(1)	0.405(8)	1.93(4)
	$\infty^3 \times 32$	0.279^{+2}_{-3}	1.33(1)		

Table 2: π and ρ masses in SU(2), in lattice units and in units of the infinite-volume string tension. The infinite volume results that are displayed for the pion in the last row are extrapolated.

We have calculated correlators for every quark bilinear J^{PC} channel. However, we find that only the $J^{PC} = 0^{-+}$ channel, corresponding to the pion, and the $J^{PC} = 1^{--}$

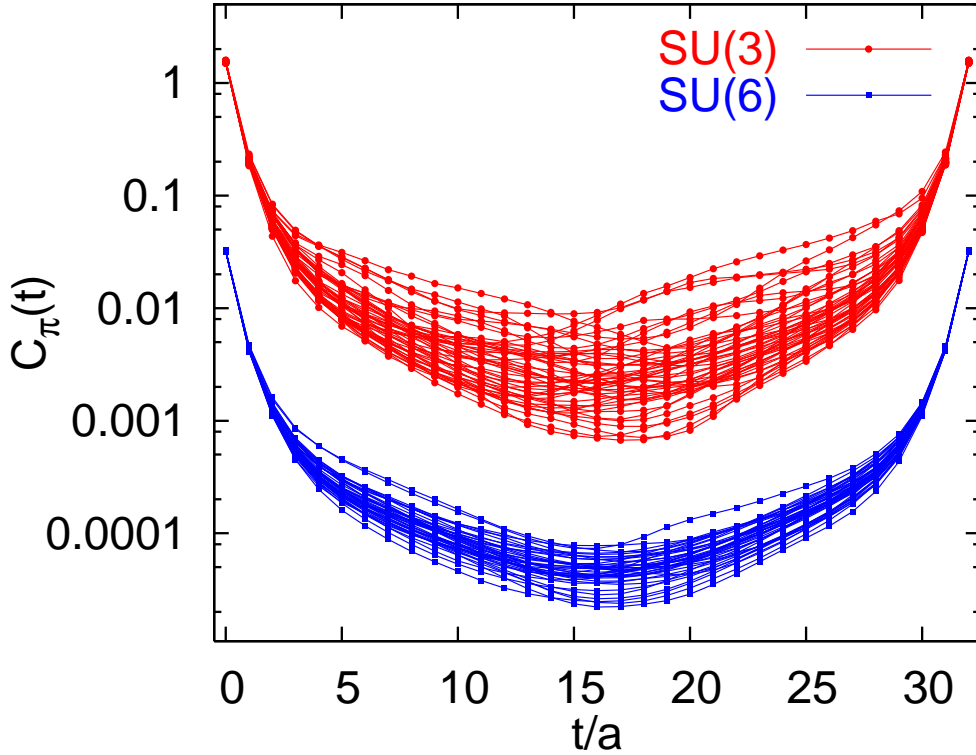


Figure 2: Point-point pseudoscalar correlators on individual $16^3 \times 32$ gauge configurations at the lightest mass values in SU(3) ($\kappa = 0.1547$, $m_\pi = 1.33(2)\sqrt{\sigma}$) and in SU(6) ($\kappa = 0.15715$, $m_\pi = 1.35(1)\sqrt{\sigma}$). The SU(6) results have been shifted vertically for the comparison.

κ	Volume	am_π	$m_\pi/\sqrt{\sigma}$	am_ρ	$m_\rho/\sqrt{\sigma}$
0.1500	$16^3 \times 32$	0.552(3)	2.64(2)	0.606(6)	2.89(3)
0.1520	$16^3 \times 32$	0.450(3)	2.15(1)	0.524(5)	2.50(2)
0.1537	$16^3 \times 32$	0.347(2)	1.66(1)	0.448(8)	2.14(4)
0.1547	$12^3 \times 32$	0.306(9)	1.46(4)	0.432(14)	2.06(7)
	$16^3 \times 32$	0.276(4)	1.32(2)	0.398(10)	1.90(5)
	$\infty^3 \times 32$	0.274^{+4}_{-9}	1.31^{+2}_{-4}		

Table 3: The same as table 2 for SU(3).

channel, corresponding to the ρ meson, have sufficiently strong signals to accurately extract masses at present statistics. We present the masses of the ground states in these channels in tables 2–5.

3.2 Finite size effects

Finite volume corrections are expected to be largest at the smallest pion masses, and at the smallest values of N . Comparing our results for the lightest π masses between different volumes (tables 2–5), we see that the differences indeed appear to decrease with N . We also see that the corrections for the ρ meson are smaller than for the π , as expected since the ρ is heavier.

κ	Volume	am_π	$m_\pi/\sqrt{\sigma}$	am_ρ	$m_\rho/\sqrt{\sigma}$
0.1520	$16^3 \times 32$	0.544(2)	2.60(1)	0.600(3)	2.87(2)
0.1540	$16^3 \times 32$	0.438(2)	2.09(1)	0.519(4)	2.48(2)
0.1554	$16^3 \times 32$	0.354(3)	1.69(1)	0.459(5)	2.19(2)
0.15625	$12^3 \times 32$	0.284(7)	1.36(3)	0.402(13)	1.92(6)
	$16^3 \times 32$	0.295(3)	1.41(1)	0.424(7)	2.02(3)
	$\infty^3 \times 32$	0.294_{-7}^{+3}	1.40_{-3}^{+1}		

Table 4: The same as table 2 for SU(4).

κ	Volume	am_π	$m_\pi/\sqrt{\sigma}$	am_ρ	$m_\rho/\sqrt{\sigma}$
0.1525	$16^3 \times 32$	0.558(2)	2.67(1)	0.618(2)	2.95(1)
0.1550	$16^3 \times 32$	0.426(2)	2.04(1)	0.507(4)	2.42(2)
0.1563	$16^3 \times 32$	0.345(2)	1.65(1)	0.447(5)	2.14(2)
0.15715	$12^3 \times 32$	0.297(4)	1.42(2)	0.420(9)	2.01(4)
	$16^3 \times 32$	0.283(2)	1.35(1)	0.416(6)	1.99(3)
	$\infty^3 \times 32$	0.282_{-8}^{+3}	1.35_{-4}^{+1}		

Table 5: The same as table 2 for SU(6).

We can estimate the infinite-volume masses by fitting our finite volume results to the form,

$$m_\pi(L) = m_\pi(\infty) [1 + C \exp(-m_\pi(\infty)L)], \quad (3.2)$$

with C positive [21, 22]. For SU(2) we have three values of L with which to carry out the fit, and we obtain $am_\pi(\infty) = 0.279_{-3}^{+2}$ and $C = 0.6_{-0.6}^{+2.1}$. Note that the data can also be fitted to a constant. For the other values of N we only have two lattice sizes for a two-parameter fit, and furthermore the $L = 12$ lattices are rather small so higher order corrections to eq. (3.2) could be substantial. Hence for these cases we take the conservative approach of assuming that the coefficient C remains constant at its SU(2) value for all SU(N). We have included the infinite-volume pion masses obtained from these fits in tables 2–5. In no case do we obtain any statistically significant deviation between the infinite volume extrapolated result and those obtained on our $L = 16a \approx 1.5$ fm lattices.

In principle we should also carry out similar corrections to the ρ meson masses. However, the corrections are much smaller for the ρ , and will be negligible compared to our statistical errors. So for the ρ we simply use the results from our largest volumes. Similarly, at larger masses it is not necessary to include finite-volume effects since they will be smaller than our statistical errors, for both the π and the ρ .

We note that our chiral extrapolations, described below, are not very sensitive to the details of our finite-volume corrections. This is because the chiral fits are mostly controlled by the data at higher mass values, which have significantly smaller errors, and are much less sensitive to potential finite-volume corrections.

3.3 Determination of the critical hopping parameter

3.3.1 κ_c at finite N

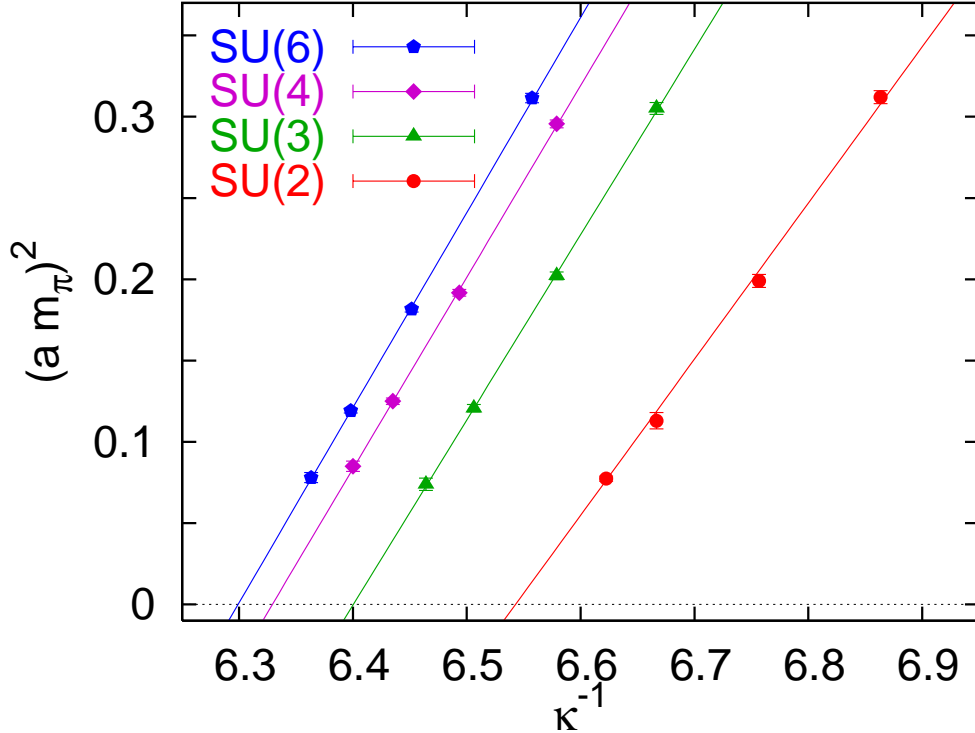


Figure 3: $(am_\pi)^2$ as a function of $1/\kappa$, eq. (3.3).

The Wilson action quark mass undergoes an additive renormalization $(2a\kappa_c)^{-1}$, see eq. (2.3). Thus we expect that the pion mass will be related to κ (up to quenched chiral logs) by,

$$(am_\pi)^2 = A \left(\frac{1}{\kappa} - \frac{1}{\kappa_c} \right). \quad (3.3)$$

By fitting to this equation we can extract κ_c for each N . We obtain good fits for each N , which we display in figure 3. Note also that the pion masses are horizontally aligned across the different N -values, indicating that we have succeeded to approximately match the κ -values to lines of constant physics, thus eliminating another possible source of systematic bias. The values of κ_c that we obtain are shown in table 6. We note that while the lattice 't Hooft coupling $2N^2/\beta$ at fixed string tension decreases with increasing N (see table 1), the κ_c -values move away from the free field limit $\kappa_{c,\text{free}} = 0.125$.

We are dealing with the quenched theory and hence eq. (3.3) should be modified by

N	κ_c	χ^2/n
2	0.1528(1)(13)	3.0
3	0.1562(1)(3)	0.9
4	0.1580(1)(4)	1.7
6	0.1588(1)(2)	1.7
∞	0.1596(2)	0.3

Table 6: The critical hopping parameter κ_c , with the reduced χ^2 of the fits. The first errors are statistical, the second systematic.

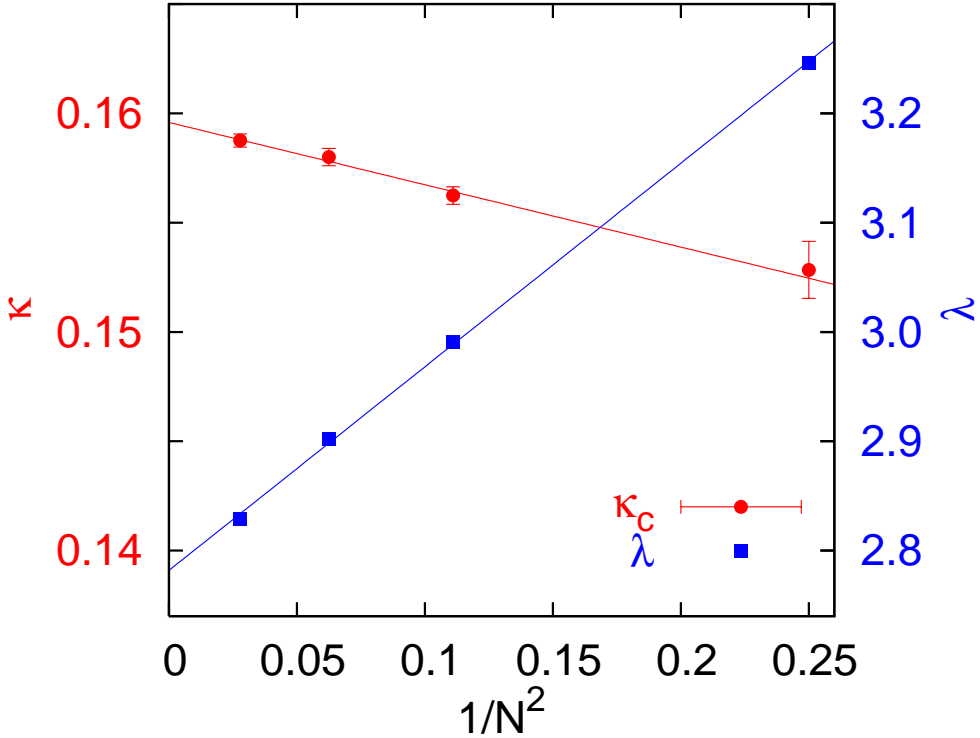


Figure 4: κ_c as a function of $1/N^2$. For comparison we also show the infinite N extrapolation of the lattice 't Hooft coupling $2N^2/\beta$.

quenched chiral logarithms [23], giving

$$(am_\pi)^2 = A' \left(\frac{1}{\kappa} - \frac{1}{\kappa_c} \right)^{1+\delta}. \quad (3.4)$$

We also fitted our results to this parametrization but have found δ to be consistent with zero, confirming that at $m_\pi > 1.3\sqrt{\sigma} \approx 580$ MeV we are not yet sensitive to quenched chiral logarithms. Comparing our best fits using eq. (3.3) to those where we allow δ to vary, we estimate the uncertainty on κ_c due to the lack of control over the chiral logs to be significantly larger than our statistical errors (see table 6). This error should decrease with N since the quenched theory will become equivalent to the unquenched theory in the large- N limit. Indeed, the $N = 2$ data allow for more curvature than the $N > 2$ data sets.

3.3.2 κ_c in the large- N limit

We expect that κ_c to have $\mathcal{O}(1/N^2)$ correction to its large- N value. Hence we fit the values of table 6 to the form,

$$\kappa_c = \kappa_c(N = \infty) + \frac{c}{N^2}. \quad (3.5)$$

After including the systematic uncertainties from the chiral extrapolation we obtain values $\kappa_c(\infty) = 0.1596(2)$ and $c = -0.028(3)$. Some of the systematics will be correlated and we obtain a rather small $\chi^2/n \approx 0.27$. We display the $1/N^2$ extrapolation of κ_c in figure 4. We also include the $1/N^2$ extrapolation of the lattice 't Hooft coupling at fixed string tension. Note that this extrapolates to the value $\lambda(N = \infty) = 2.780(4)$.

3.4 The ρ meson mass

3.4.1 m_ρ at finite N

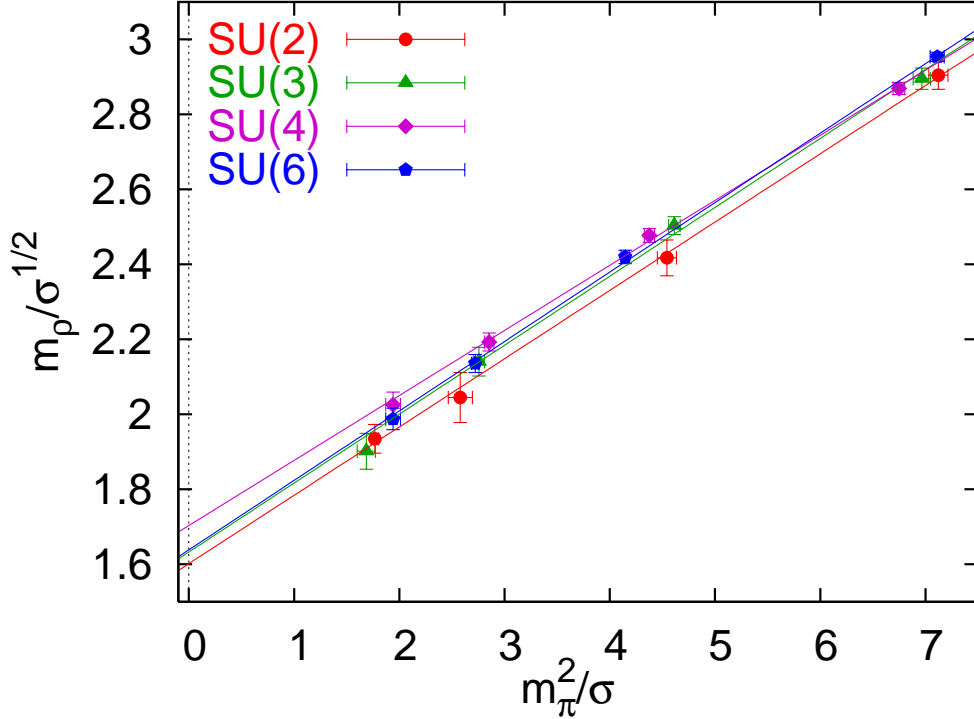


Figure 5: Fits of $m_\rho/\sqrt{\sigma}$ as functions of m_π^2/σ , eq. (3.6), at different N .

In chiral perturbation theory, as well as in the heavy quark limit, m_ρ depends linearly on the quark mass m_q . Within our range of pion masses $m_\pi/\sqrt{\sigma} \approx 1.3 \dots 2.6$ we find m_π^2 to linearly depend on κ^{-1} and therefore to be proportional to the quark mass. Hence, we can fit our ρ masses to the parametrization,

$$\frac{m_\rho}{\sqrt{\sigma}} = \frac{m_\rho(0)}{\sqrt{\sigma}} + B \frac{m_\pi^2}{\sigma}, \quad (3.6)$$

where $m_\rho(0)$ denotes the ρ meson mass in the chiral limit. Quenched chiral logarithms will modify the relationship between m_q and m_π^2 , however eq. (3.6) remains valid [23].

We obtain good fits in each case, which we show in figure 5. We display corresponding parameter values $m_\rho(0)/\sqrt{\sigma}$ and B in table 7.

3.4.2 m_ρ in the large- N limit

In the quenched approximation the parameters $m_\rho(0)/\sqrt{\sigma}$ and B are each expected to have $\mathcal{O}(1/N^2)$ corrections to their large- N values, in analogy to eq. (3.5). We see from figure 5

N	$m_\rho(0)/\sqrt{\sigma}$	B	χ^2/n
2	1.60(5)	0.182(10)	0.2
3	1.63(4)	0.184(9)	1.0
4	1.70(3)	0.174(6)	0.5
6	1.64(3)	0.185(4)	0.6

Table 7: The fit parameters of eq. (3.6) for each N , with the reduced χ^2 -values.

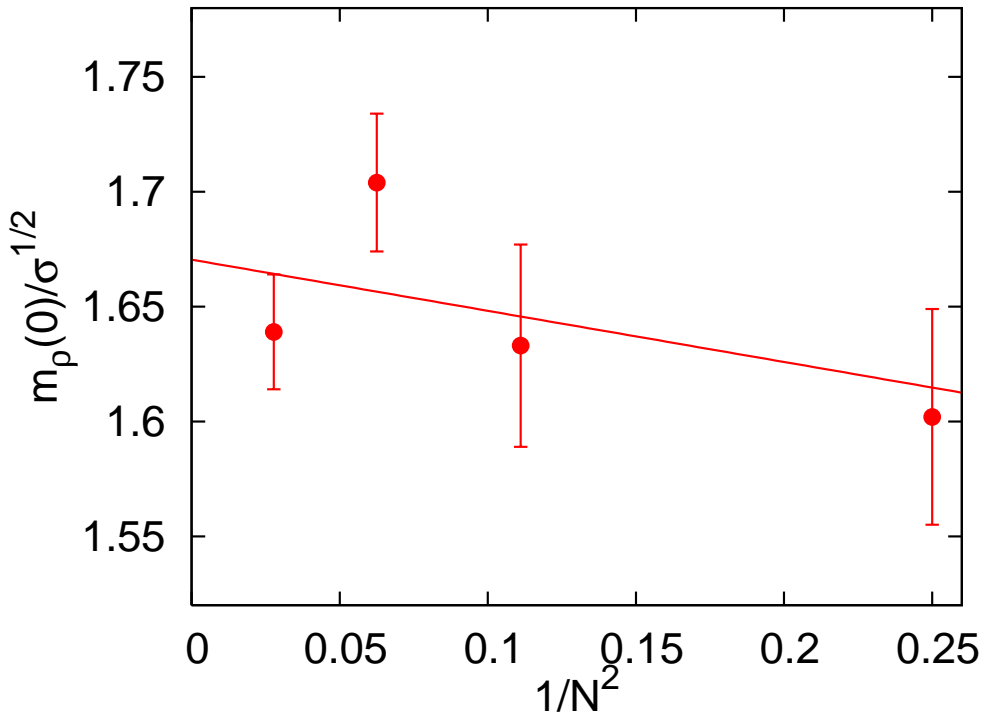


Figure 6: $m_\rho/\sqrt{\sigma}$ in the chiral limit, as a function of $1/N^2$.

that the results and fits for different N are all very similar, with all points nearly lying on one line, so these corrections should be small. We obtain,

$$m_\rho(0)/\sqrt{\sigma} = 1.670(24) - \frac{0.22(23)}{N^2}, \quad (3.7)$$

and

$$B = 0.182(5) - \frac{0.01(5)}{N^2}. \quad (3.8)$$

The fits are both good, with reduced χ^2 -values of 1.8 and 1.3, respectively. We plot the fit for $m_\rho(0)/\sqrt{\sigma}$ in figure 6. Note that the N -dependence is extremely small both for $m_\rho/\sqrt{\sigma}$ and for B . In particular, the difference between $m_\rho(0)$ for SU(3) and SU(∞) amounts to only (1.4 ± 1.6) %.

Equating $\sqrt{\sigma} \approx 444$ MeV, the large- N chiral ρ mass, eq. (3.7), corresponds to,

$$m_\rho(m_\pi = 0, N = \infty) \approx 741(11)\text{MeV}. \quad (3.9)$$

The above value $\sigma \approx 1$ GeV/fm is motivated by Regge trajectories, potential model fits to quarkonium spectra and unquenched $N = 3$ lattice data [24]. However, there is a systematic uncertainty associated with it, in particular also since the QCD string at finite N and $n_F > 0$ will decay, once a critical distance is reached [25]. Moreover, no $N = \infty$ experiment exists. Nonetheless, we find it interesting that this mass-prediction for the stable $N = \infty$ ρ meson comes close to the mass $m_\rho \approx 775$ MeV of the experimental ρ resonance, which in fact has a significant decay width, $\Gamma \approx 150$ MeV. Note that at physical

π mass we obtain the large- N limit $m_\rho \approx 749(11)$ MeV. The (unknown) scale uncertainty from the string tension is not included in the above error estimates and neither are finite lattice spacing effects. The continuum limit extrapolation of section 4 below increases our large- N m_ρ prediction by another ≈ 45 MeV.

3.5 Excited states

In principle, our correlation matrices enable us to extract the masses of excited states as well as of the ground states. However, in practice we obtain poor mass plateaus for the excited states, and our statistical errors are rather large. Having said that, our results are consistent with the first excited pseudoscalars and vectors having no N -dependence at the 10 % level. Also, we find that our correlators at a given pion mass are similar for all N , not just at large t where they are dominated by the ground state, but all the way back to $t = 0$ where many excited states contribute. An example of this can be seen in figure 2. This is consistent with the entire spectrum of excited states to only weakly depend on N . The correlators also depend on the overlaps of our operators with the excited states, and these overlaps in turn depend on wavefunctions of the excited states. So this also suggests that the meson sizes and internal properties do not change strongly with N .

4. The continuum limit

Presumably there are lattice spacing corrections to our results. We can get some idea of their size from the study of Del Debbio *et al.* [13], on somewhat coarser lattices.

Turning first to the large- N limit of their results, and using the facts that their lattice spacing is given by $a \approx 1/(5T_c)$, where T_c denotes the de-confinement temperature, and that at $N = \infty$ one has $T_c/\sqrt{\sigma} \approx 0.5970$ [15], they obtain,

$$\frac{m_\rho}{\sqrt{\sigma}} = 1.609(9) + 0.1750(3) \frac{m_\pi^2}{\sigma} \quad ; \quad a\sqrt{\sigma} = 0.3350. \quad (4.1)$$

We can compare this to our large- N result, eqs. (3.6)–(3.8),

$$\frac{m_\rho}{\sqrt{\sigma}} = 1.670(24) + 0.182(5) \frac{m_\pi^2}{\sigma} \quad ; \quad a\sqrt{\sigma} = 0.2093. \quad (4.2)$$

We see that, despite the 60 % difference in lattice spacings, the results for both the chiral limit and the slope of the ρ mass are very similar, differing by less than 5 %. Also the ratio of our and their results remains remarkably independent of the π mass, when expressed in units of σ .

The leading lattice artefacts are of order a and a simple linear extrapolation yields,

$$\frac{m_\rho}{\sqrt{\sigma}} = 1.77(5) + 0.193(14) \frac{m_\pi^2}{\sigma} \quad ; \quad (a \rightarrow 0). \quad (4.3)$$

Obviously, with just two values of the lattice spacing, we have little control over the systematics of this continuum limit extrapolation. Therefore we also attempt a purely quadratic extrapolation in a and find the central values 1.70 and 0.186 for the two above parameters,

respectively. Based on this and results of previous large scale $N = 3$ quenched spectroscopy studies with Wilson action [9], that included similar lattice spacings (as well as finer ones), we conclude that the statistical errors stated above are sufficiently large to accommodate the possible contributions from subleading terms.

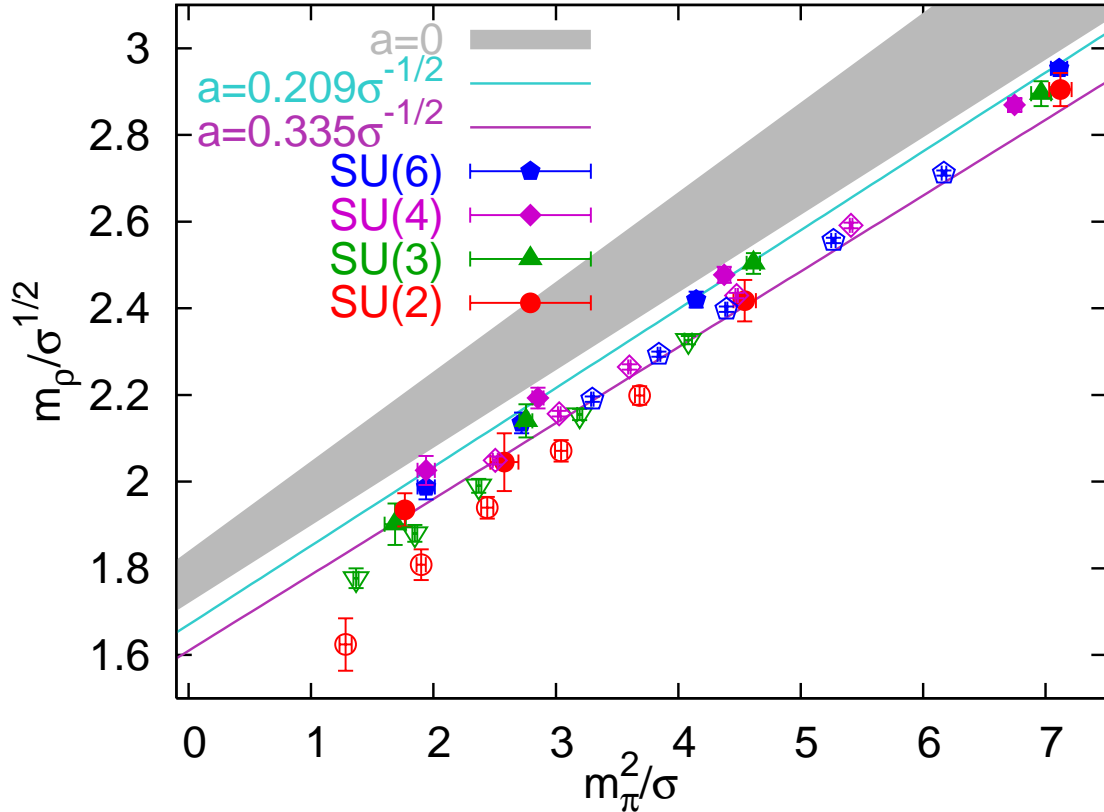


Figure 7: Results for $m_\rho/\sqrt{\sigma}$ and m_π^2/σ from this work (full symbols, $a \approx 0.209/\sqrt{\sigma}$) and from ref. [13] (open symbols, $a = 0.2/T_c \approx 0.335/\sqrt{\sigma}$). The lines correspond to the respective $N \rightarrow \infty$ limits and the grey error band denotes our large- N continuum limit estimate eq. (4.3).

We now turn to the finite- N corrections. Here the two sets of results appear to be rather different. Our results show a very weak N -dependence, with for example the difference between $m_\rho(0)$ for SU(3) and SU(∞) being only (1.4 ± 1.6) %. The corresponding value of ref. [13] is (12.8 ± 0.6) %, much larger. Most of this difference can be attributed to the different ways of setting the scale; the ratio $T_c/\sqrt{\sigma}$ depends on N [15]. To remove this effect we have rescaled the results of ref. [13], using the appropriate values of $T_c/\sqrt{\sigma}$ for each N [15]. We compile all these results in figure 7. Again we remark that the results of ref. [13] were obtained at different values of $a\sqrt{\sigma}$ for the different N . Also note that the range of pion masses covered in this case varies with N . Nevertheless, we see that when plotted in this way the two studies agree very closely, with the exception of SU(2). This suggests that most of the difference between the two data sets is due to the different methods of setting the scale, rather than from lattice corrections. The finite lattice spacing effects might be larger for SU(2), accounting for the deviation there.

The fact that the N -dependence at our finer lattices is already consistent with zero leaves little room for $1/N^2$ corrections to $m_\rho/\sqrt{\sigma}$ being larger than 3 % at $N = 3$, at least for pion masses $m_\pi/\sqrt{\sigma} < 2.6$. The figure also contains the large- N extrapolations of the data sets at the two lattice spacings and our continuum limit estimate eq. (4.3) (grey error band).

All this suggests that our finite- a results deviate by no more than 5–10 % from the continuum limit. This is true both for the large- N limit, eq. (4.2), and for the finite- N corrections. Also, these corrections are smaller when the masses are expressed in terms of the string tension than when they are expressed in terms of the de-confinement temperature. Note that this is opposite to the situation with respect to the scalar glueball which scales better between different N when normalized with respect to T_c , rather than by $\sqrt{\sigma}$ [5].

5. Summary and Discussion

We have studied the ρ and π meson masses in quenched $SU(N)$ QCD with $N = 2, 3, 4, 6$ at one value of the lattice spacing $a\sqrt{\sigma} = 0.2093$, in units of the string tension, at four different values of the quark mass. Our main result can be summarized by combining eqs. (3.6), (3.7) and (3.8), giving

$$\frac{m_\rho(m_\pi)}{\sqrt{\sigma}} = 1.670(24) - \frac{0.22(23)}{N^2} + \left(0.182(5) - \frac{0.01(5)}{N^2}\right) \frac{m_\pi^2}{\sigma}. \quad (5.1)$$

Combining our data with that of Del Debbio *et al.* [13], allows us to extrapolate the large- N result to the continuum limit, see eq. (4.3).

We can compare our results to predictions from AdS/QCD correspondence. As an example, we consider the case of the Constable-Myers deformation [26] analyzed in ref. [4]. Reconverting their prediction into their original units of $m_\rho(0)$ this reads,

$$\frac{m_\rho(m_\pi)}{m_\rho(0)} \approx 1 + 0.338 \left(\frac{m_\pi}{m_\rho(0)}\right)^2. \quad (5.2)$$

At our value of a we obtain 0.304(3) for this slope in units of $m_\rho(0)$, while the values obtained in ref. [13] can be translated into a coefficient 0.2816(2). A linear continuum limit extrapolation of these two numbers yields 0.341(4) and a quadratic extrapolation results in 0.318(3). The expected dominant behaviour is linear and hence we quote 0.341 ± 0.023 as our large- N continuum limit result, where the error is dominated by the systematics of the continuum limit extrapolation. This agrees remarkably well with the above AdS/QCD prediction eq. (5.2).

In the large- N limit the quenched theory is equivalent to the full, unquenched, theory. We have found that the $\mathcal{O}(1/N^2)$ quenched corrections to the large- N result are very small. What about the $\mathcal{O}(n_F/N)$ corrections of the unquenched theory? We can get an idea of their size without needing to carry out full unquenched simulations, by comparing our results with experiment. Converting the $a \rightarrow 0$ and $N \rightarrow \infty$ extrapolated result of eq. (4.3) into physical units gives,

$$m_\rho(m_\pi) = (786 \pm 22) \text{ MeV} + (435 \pm 34) \frac{m_\pi^2}{\text{GeV}}. \quad (5.3)$$

At physical π mass this yields an infinite N value, $m_\rho = (794 \pm 23)$ MeV, in perfect agreement with experiment: $m_\rho \approx 775$ MeV. This suggests that not only the quenched $1/N^2$ -corrections but also the unquenched n_F/N -corrections are small at $N = 3$.

Of course the string tension value $\sqrt{\sigma} = 444$ MeV is arbitrary and we did not associate any error to this choice. Still this is very encouraging and might explain the success of the quenched approximation in light hadron spectroscopy calculations of the 1980s and 90s [9]. It is certainly worthwhile to extend the present study to other mesonic channels, to confirm this picture.

As discussed above, the fact that our results agree reasonably well with those of ref. [13] although our lattice spacings differ by as much as 60 % suggests that the systematic error due to the finite lattice spacing is already small at $a \approx 0.093$ fm for the Wilson action. Our continuum limit extrapolation confirms it to be smaller than 10 %. It would be nice to further constrain the continuum limit by repeating our work with the same analysis methods at another, smaller, lattice spacing.

The errors associated with the neglect of quenched chiral logs in our pion mass fits could be reduced by going to lighter π masses; the obstacle of exceptional configurations should be reduced at high N since the Dirac matrix eigenvalue distribution becomes narrower [12]. Our calculations have been carried out on more than one volume, so we already have some control over the small finite volume corrections. These should in any case disappear in the large- N limit.

We have not been able to obtain accurate masses for excited states in this work, although our results do suggest that they do not have a strong N -dependence. We intend to use improved meson operators to calculate the masses of the low-lying excited states more accurately in the future. This should yield several independent mass ratios in the large- N limit which can be used to constrain AdS/QCD models. This would also shed more light on the question if the use of the quenched approximation at $n_F/N = 3/3$ is justifiable from a large- N viewpoint and relate low energy constants in chiral Lagrangians. We are also planning to study the scalar sector and flavour singlet diagrams.

Acknowledgments

We thank Johanna Erdmenger and Biagio Lucini for discussions. The computations were mainly performed on the Regensburg QCDOC machine and we thank Stefan Solbrig for keeping this alive. This work is supported by the EC Hadron Physics I3 Contract RII3-CT-2004-506087 and by the GSI University Program Contract RSCHAE. F.B. is supported by the STFC.

References

- [1] J. M. Maldacena, *The large N limit of superconformal field theories and supergravity*, *Adv. Theor. Math. Phys.* **2** (1998) 231, [hep-th/9711200](#).
- [2] U. Gursoy and E. Kiritsis, *Exploring improved holographic theories for QCD: part I*, *J. High Energy Phys.* **0802** (2008) 032, [arXiv:0707.1324 \[hep-th\]](#).

- [3] U. Gursoy, E. Kiritsis and F. Nitti, *Exploring improved holographic theories for QCD: part II*, *J. High Energy Phys.* **0802** (2008) 019, [arXiv:0707.1349 \[hep-th\]](#).
- [4] J. Erdmenger, N. Evans, I. Kirsch and E. Threlfall, *Mesons in gauge/gravity duals — A review*, *Eur. Phys. J. A* **35** (2008) 81, [arXiv:0711.4467 \[hep-th\]](#).
- [5] B. Lucini, M. Teper and U. Wenger, *Glueballs and k-strings in SU(N) gauge theories: calculations with improved operators*, *J. High Energy Phys.* **0406** (2004) 012, [hep-lat/0404008](#).
- [6] B. Lucini and G. Moraitis, *The running of the coupling in SU(N) pure gauge theories*, [arXiv:0805.2913 \[hep-lat\]](#).
- [7] B. Lucini, M. Teper and U. Wenger, *The high temperature phase transition in SU(N) gauge theories*, *J. High Energy Phys.* **0401** (2004) 061, [hep-lat/0307017](#).
- [8] G. 't Hooft, *A planar diagram theory for strong interactions*, *Nucl. Phys.* **B 72** (1974) 461.
- [9] S. Aoki *et al.* [CP-PACS Collaboration], *Quenched light hadron spectrum*, *Phys. Rev. Lett.* **84** (238) 2000, [hep-lat/9904012](#).
- [10] S. Scherer, *Introduction to chiral perturbation theory*, *Adv. Nucl. Phys.* **27** (2003) 277, [hep-ph/0210398](#).
- [11] J. Kiskis, R. Narayanan and H. Neuberger, *Proposal for the numerical solution of planar QCD*, *Phys. Rev.* **D 66** (2002) 025019, [hep-lat/0203005](#).
- [12] G. Bali and F. Bursa, *Meson masses at large N_c* , *PoS LATTICE2007* (2006) 050 [arXiv:0708.3427 \[hep-lat\]](#).
- [13] L. Del Debbio, B. Lucini, A. Patella and C. Pica, *Quenched mesonic spectrum at large N*, *J. High Energy Phys.* **0803** (2008) 062, [arXiv:0712.3036 \[hep-th\]](#).
- [14] R. Edwards and B. Joó [SciDAC Collaboration], *The Chroma software system for lattice QCD*, *Nucl. Phys.* **140** (Proc. Suppl.) (2005) 832, [hep-lat/0409003](#).
- [15] B. Lucini, M. Teper and U. Wenger, *Properties of the deconfining phase transition in SU(N) gauge theories*, *J. High Energy Phys.* **0502** (2005) 033, [hep-lat/0502003](#).
- [16] J. Kiskis, R. Narayanan and H. Neuberger, *Does the crossover from perturbative to nonperturbative physics in QCD become a phase transition at infinite N?*, *Phys. Lett.* **B 574** (65) 2003, [hep-lat/0308033](#).
- [17] C. Alexandrou, F. Jegerlehner, S. Güsken, K. Schilling and R. Sommer, *B meson properties from lattice QCD*, *Phys. Lett.* **B 256** (1991) 60.
- [18] M. Albanese *et al.* [APE Collaboration], *Glueball masses and string tension in lattice QCD*, *Phys. Lett.* **B 192** (1987) 163.
- [19] C. Michael, *Adjoint sources in lattice gauge theory*, *Nucl. Phys.* **B 259** (1985) 58.
- [20] M. Lüscher and U. Wolff, *How to calculate the elastic scattering matrix in two-dimensional quantum field theories by numerical simulation*, *Nucl. Phys.* **B 339** (1990) 222.
- [21] G. Colangelo, A. Fuhrer and C. Haefeli, *The pion and proton mass in finite volume*, *Nucl. Phys.* **153** (Proc. Suppl.) (2006) 41, [hep-lat/0512002](#).
- [22] G. Colangelo and S. Dürr, *The pion mass in finite volume*, *Eur. Phys. J.* **C 33** (2004) 543, [hep-lat/0311023](#).

- [23] S. R. Sharpe, *Quenched chiral logarithms*, *Phys. Rev. D* **46** (1992) 3146, [hep-lat/9205020](#).
- [24] G. S. Bali *et al.* [T χ L Collaboration], *Static potentials and glueball masses from QCD simulations with Wilson sea quarks*, *Phys. Rev. D* **62** (2000) 054503, [hep-lat/0003012](#).
- [25] G. S. Bali, H. Neff, T. Düssel, T. Lippert and K. Schilling [SESAM Collaboration], *Observation of string breaking in QCD*, *Phys. Rev. D* **71** (2005) 114513, [hep-lat/0505012](#).
- [26] N. R. Constable and R. C. Myers, *Exotic scalar states in the AdS/CFT correspondence*, *J. High Energy Phys.* **9911** (1999) 020, [hep-th/9905081](#).